DISTRIBUTIONS IN $b \to s \ell^+ \ell^-$ and MODEL-INDEPENDENT ANALYSIS

GUDRUN HILLER
(CERN | MUNICH)

Joint meeting LHCb | theory Dec 3, 2004

outline:

I hadronic invariant mass spectrum and cuts

based on: hep-ph/9803407 [HQET]
hep-ph/9803428 [HQET + Fermi motion (FM)]
hep-ph/9807418 [FM + $c\bar{c}$-BGD]

II (more) model-independent analysis and New Physics (NP) searches

mostly using hep-ph/0112300
hep-ph/0310219

INCLUSIVE $B \to X_s \ell^+ \ell^-$ DECAYS and CUTS

inclusive decays – theoretically clean; from OPE
– experimentally difficult $\to$
cuts required to suppress BGD
(similar to $b \to s\gamma$, $b \to u \ell \nu$ decays)

- cuts in $q^2 = (p_{\ell^+} + p_{\ell^-})^2$ to remove J/ψ, ψ'
  $\to$ low / high $-q^2$ window (see Tobias' Talk)

- BGD from double semileptonic

$$\left.\begin{array}{l} b \to c\, e^- \bar{\nu} \\ \quad \hookrightarrow s\, e^+ \nu \end{array}\right\} = s\, e^+ e^- + \text{missing energy}$$

suppress but cut on invariant mass of X_s

e.g. $m_{X_s} \leq 2.1$ GeV (Belle)

$\Rightarrow$ need to calculate $\frac{d\Gamma}{dm_{X_s}}(B \to X_s \ell\ell)$

more specifically, we (ONLY) need for efficiency

$$\varepsilon_{X_s} = \frac{\int_{\text{CUT}} dm_{X_s} \frac{d\Gamma}{dm_{X_s}}}{\int_{\text{FULL}} dm_{X_s} \frac{d\Gamma}{dm_{X_s}}}$$

HADRONIC INVARIANT MASS SPECTRUM

$$m_{X_s}^2 = (p_B - q)^2 \quad \text{hadron}$$
$$s_0 = (p_b - q)^2 \quad \text{parton}$$
level

- lowest order parton level $\frac{d\Gamma}{ds_0} \sim \delta(s_0 - m_s^2)$

- α_s-corrections (Bremsstrahlung) $b \to \underbrace{s+g}\, \ell^+\ell^-$

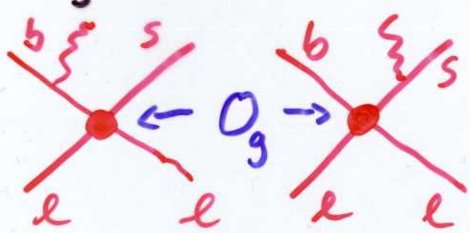

$m_s^2 \le s_0 \le m_b^2$

NLO, also Sudakov resummation

- non-perturbative effects I phase space

$m_B - m_b = \bar\Lambda$

generate non-trivial spectrum already at α_s^0: $s_0 = m_s^2$

$$m_{X_s}^2 = \bar\Lambda^2 + 2\bar\Lambda(m_b - E_q) + s_0$$

physical spectrum $m_K^2 \le m_{X_s}^2 \le m_B^2$

OPE valid ~~for~~ $m_{X_s}^2 \ge m_B \bar\Lambda$

Belle cut: $2.1\,\text{GeV} \sim O(m_B\bar\Lambda) \ge m_{X_s}^2$

"Shapefunction and resonance region"

II b moves within B (Fermi-motion)

Gaussian momentum distribution around $p_F \approx O(\bar\Lambda)$

fit parameters to $B \to X_s\gamma$ photon energy spectrum

$\hookrightarrow$ $p_F = 410$ MeV hep-ex/0108032 (CLEO)

→ FIG

hadronic invariant mass cuts

Belle'02 $b \to s\ell^+\ell^-$ analysis $m_{X_s} < 2.1$ GeV $\qquad$ m_{X_s}-spectrum:

bremsstrahlung and Fermi motion (b-quark moves in B-meson with p_F)

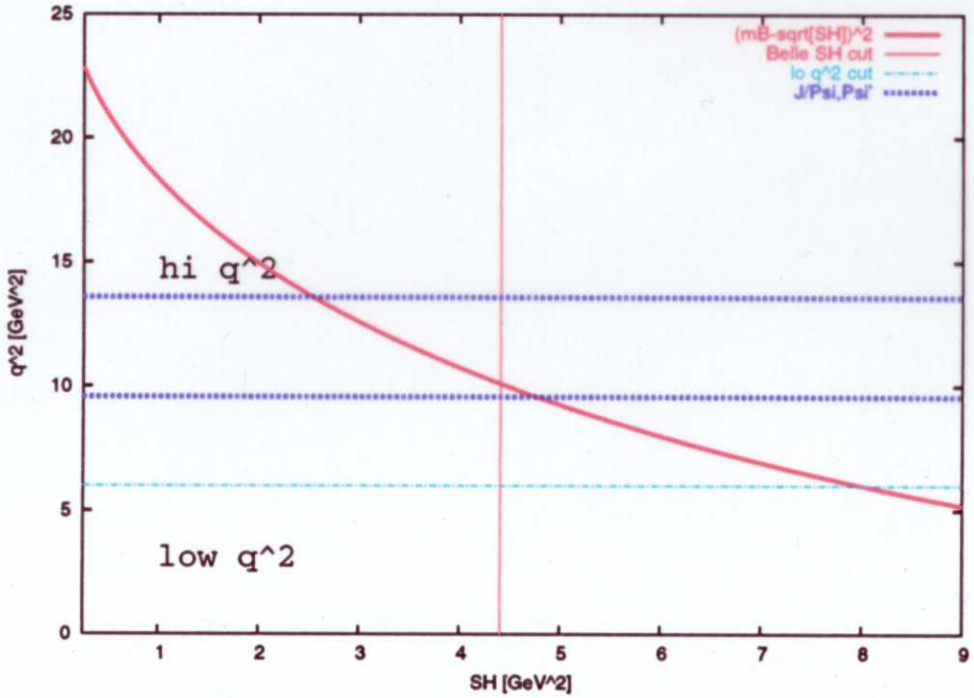

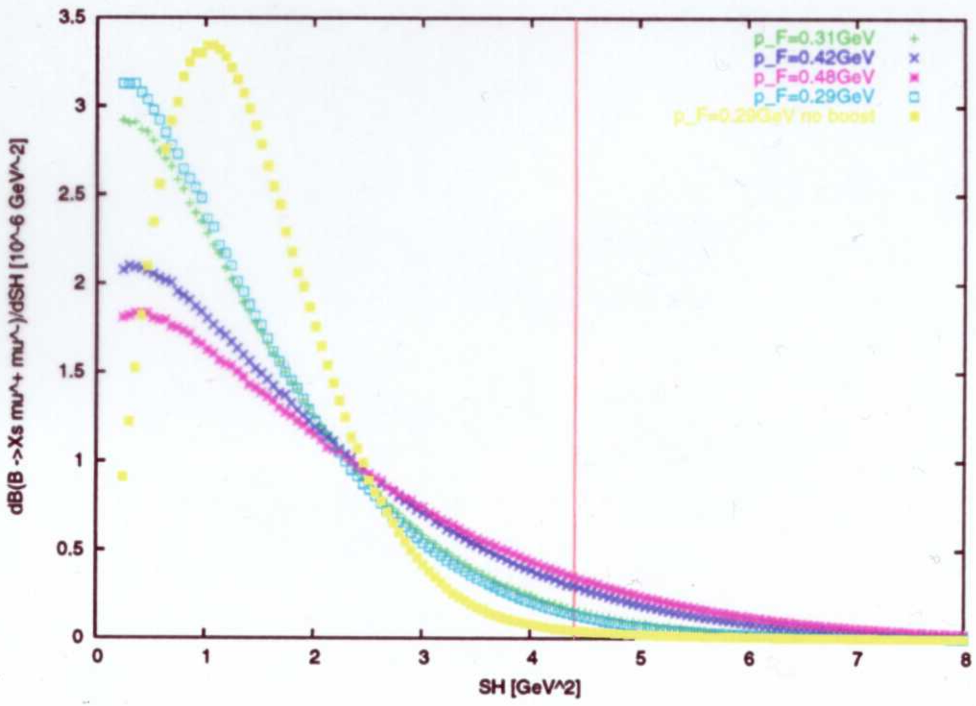

efficiency in Fermi mo $(\int_{m_K}^{2.1GeV} dX_s \frac{dBr}{dX_s})/Br = 93 \pm 4\%$ hep-ph/9807418

fit $\bar{B} \to X_s\gamma$ photon spectrum by CLEO hep-ex/0108032: $p_F = 410$ MeV

COMMENTS ON $\frac{d\Gamma}{dm_{X_s}}$ and PHASE SPACE

- Resonance peaks are not captured, spectrum works only in "duality" sense, i.e. sufficiently smeared over m_{X_s} region

$$\left[X_s = K + n\pi,\ K^* + n\pi,\ \Lambda \bar{p} + n\pi, \ldots \qquad n = 0, 1, \ldots 35 \right]$$

large $m_{X_s}^2 \gtrsim m_B \bar{\Lambda}$ => large # final states

- efficiency ε_{X_s} not sensitive to FM-parameters

$$\boxed{\varepsilon_{X_s} = 93 \pm 4\,\%} \quad \text{for } m_{X_s} < 2.1\,\text{GeV}$$

- Alternatively, Breit-Wigner K, K* and add to "continuum" above resonances

$$\frac{d\Gamma}{dm_{X_s}^2} = BW(K, K^*) + \Theta(m_{X_s}^2 - m_{\text{CONT.}}^2)\frac{d\Gamma}{dm_{X_s}^2}$$

with branching ratio from data

- 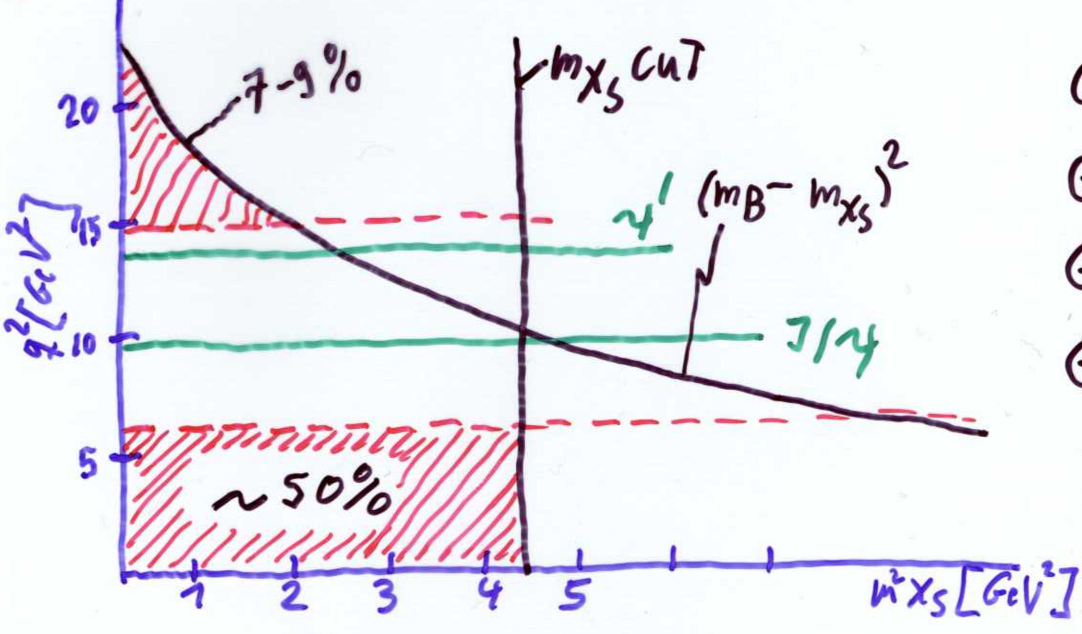

Low-q^2 region

⊕ $C_7 - C_9$ interference

⊕ $c\bar{c}$ BGD

⊕ many events

⊖ not optimal cut

NEW PHYSICS in $b \to s \ell^+ \ell^-$ TRANSITIONS

$b \to s \ell^+ \ell^-$ in SM

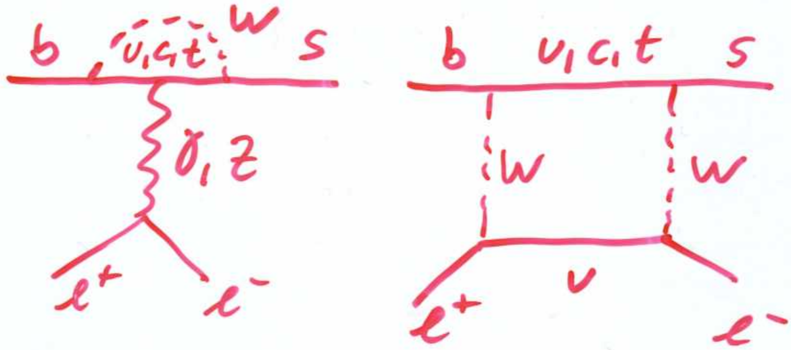

$$H_{eff} = -\frac{4 G_F}{\sqrt{2}} V_{tb} V_{ts}^* \sum_i C_i O_i$$

dipole : $O_7 \sim m_b \bar{s}_L \sigma_{\mu\nu} b_R F^{\mu\nu}$; $O_8 \sim m_b \bar{s}_L \sigma_{\mu\nu} b_R G^{\mu\nu}$

4-Fermi : $O_9 \sim \bar{s}_L \gamma_\mu b_L \bar{\ell} \gamma^\mu \ell$; $O_{10} \sim \bar{s}_L \gamma_\mu b_L \bar{\ell} \gamma^\mu \gamma_5 \ell$

Z-penguins and box also in $b \to s \nu \bar{\nu}$, $b \to s q \bar{q}$

BEYOND THE SM $\quad C_i \to C_i^{SM} + C_i^{NP}$

AND/OR $\quad$ new operators

e.g. helicity flipped $O_i' = (O_i$ with $L \leftrightarrow R)$

in SM (and MFV) : $C_i' = \frac{m_s}{m_b} C_i$

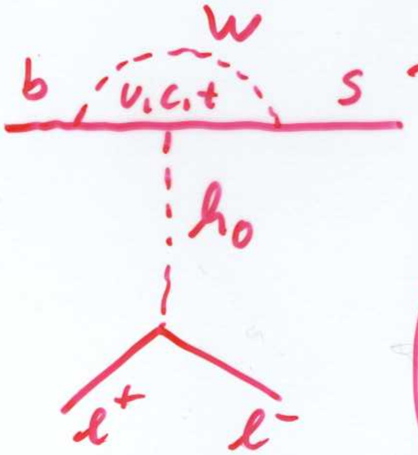

scalar/pseudoscalar

$O_S \sim \bar{s}_L b_R \bar{\ell} \ell$

$O_P \sim \bar{s}_L b_R \bar{\ell} \gamma_5 \ell$

$C_{S/P}^{SM} \sim \frac{m_\ell m_b}{m_W^2}$ tiny even for τ

MORE MODEL-INDEPENDENT ANALYSIS

$B \to K, K^*, X_s\, \ell^+\ell^-$ - spectra = function$(\underbrace{C_7^{eff}, C_9, C_{10}^{eff}}_{\text{SM basis}}, \underbrace{C_S, C_P}_{\text{extended}})$

in general even more ; practically undoable

ANALYSIS STATUS:

- constraints on dipole operators O_7, O_8 from $b \to s\gamma$, $b \to s g$
  $\to$ Fig lowest order $Br(B \to X_s \gamma) \sim |C_7^{eff}|^2$
  $\to C_7^{eff} \simeq \pm C_{7\,SM}^{eff}$
- O_S, O_P constrained by $Br(B_s \to \mu^+\mu^-)$

$$\sqrt{|C_S|^2 + |C_P + \delta_{10}|^2} \leq 1.6 \left[\frac{Br(B_s \to \mu\mu)}{5.3 \cdot 10^{-7}}\right] \leftarrow \text{CDF bound RUN II}$$

iFF e.g. neutral Higgs induced : $C_{S,P} \sim m_\ell$

$\Rightarrow$ enters differently in $b \to s \mu^+\mu^-$ and $b \to s e^+e^-$

use SAME cuts for both $\mu\mu$ and ee modes

$$R_H \equiv \frac{\int \frac{d\Gamma}{dq^2}(B \to H\mu\mu)}{\int \frac{d\Gamma}{dq^2}(B \to H e e)} \qquad H = K, K^*, X_s$$

clean ! $R_H^{SM} = 1 + \mathcal{O}\left(\frac{m_\mu^2}{m_b^2}\right)$

room for NP : R_K up to $\mathcal{O}(10\%)$

R_{K^*, X_s} up to $\mathcal{O}(5-8\%)$

correlated with $Br(B_s \to \mu^+\mu^-)$ $\to$ FIG

FROM hep-ph/0310219

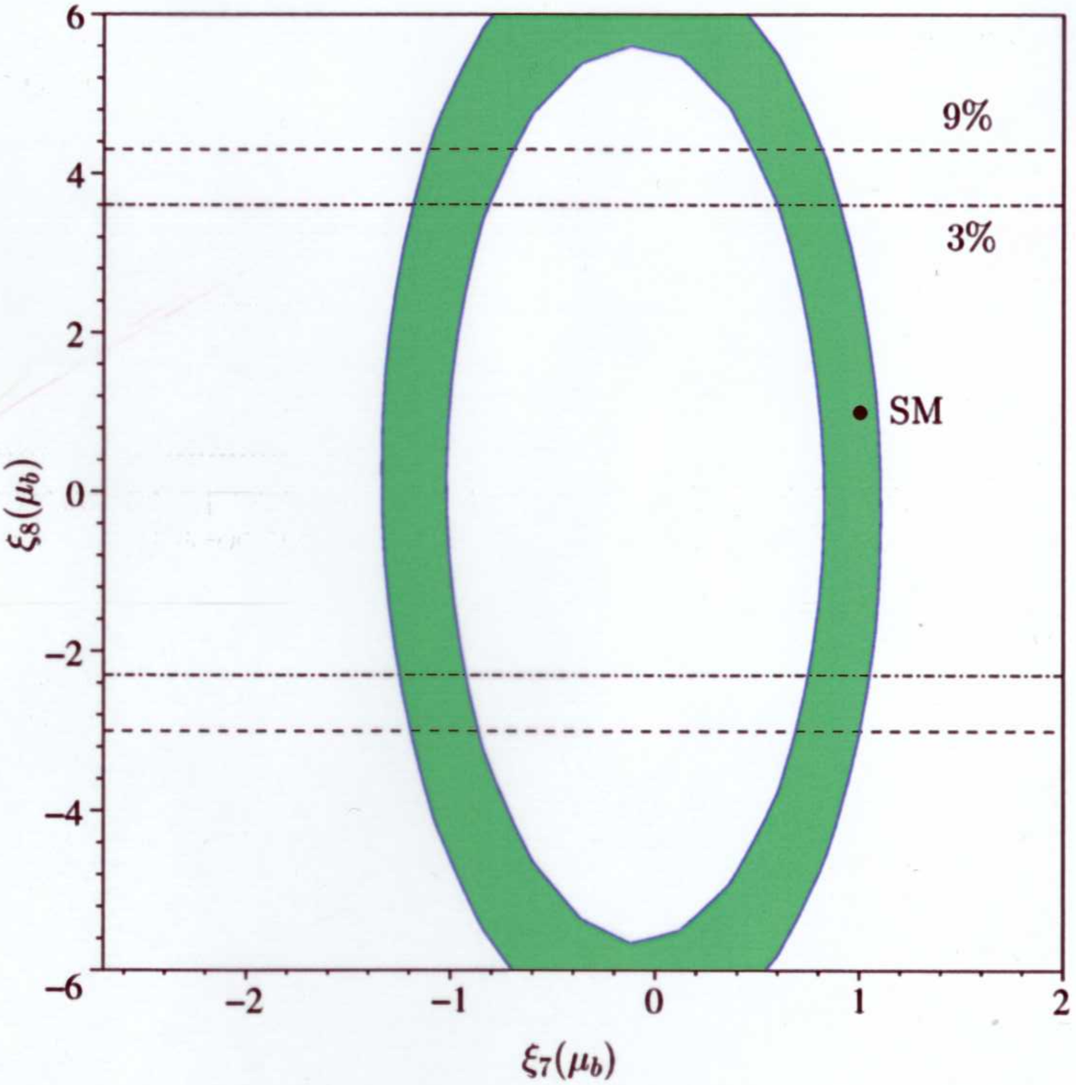

$$\xi_i = \frac{C_i^{SM} + C_i^{NP}}{C_i^{SM}}$$

FROM hep-ph/0310219

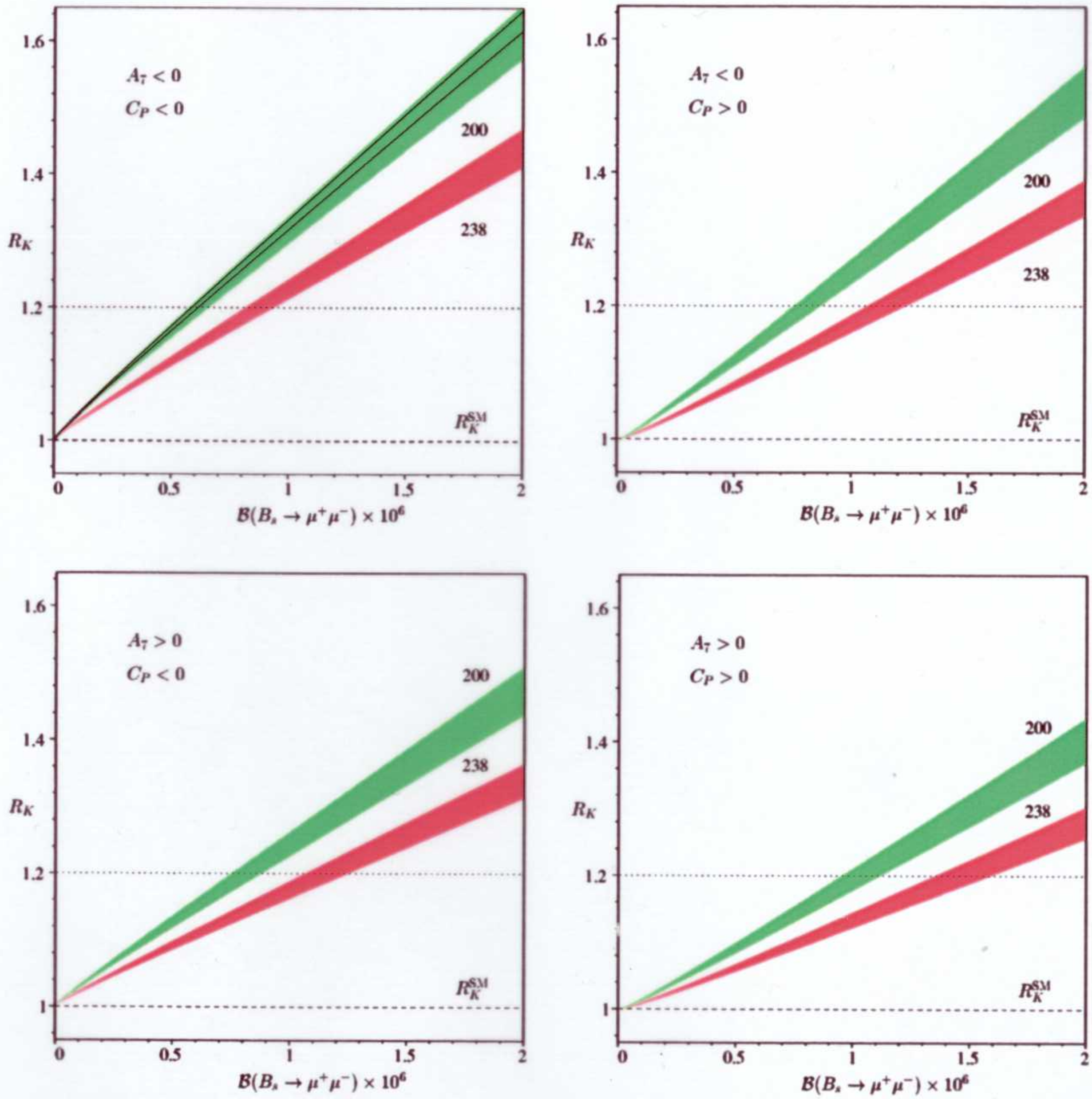

Figure 4: Correlation between R_K and the $B_s \to \mu^+\mu^-$ branching ratio for different signs of A_7 and C_P, two values of f_{B_s} in MeV and $A_{9,10} = A_{9,10}^{\rm SM}$. The shaded areas have been obtained by varying the $B \to K$ form factors according to Ref. [10] and A_7 as given in Eq. (4.6). In the upper left plot, the form factor uncertainty is illustrated for fixed $A_7 = A_7^{\rm SM}$ and $f_{B_s} = 200$ MeV by solid lines. The dotted lines correspond to the 90% C.L. upper limit on R_K in Eq. (2.10). Dashed lines denote the SM prediction for R_K.

- Bounds on O_9, O_{10} from $b \to s \ell\ell$ decays; also in the presence of NP in $C_{S,P}$ and C_7, C_8 [quite involved] → FIG

VERY USEFUL, BUT NO DATA SO FAR:
[very early ones by Belle on $A_{FB}(B \to K^* \ell\ell)$]
hep-ex/0410006

Forward - Backward asymmetry:

$$A_{FB}(B \to K^*, X_s \mu\mu) \sim C_{10} \cdot (C_7 + \dots C_9)$$

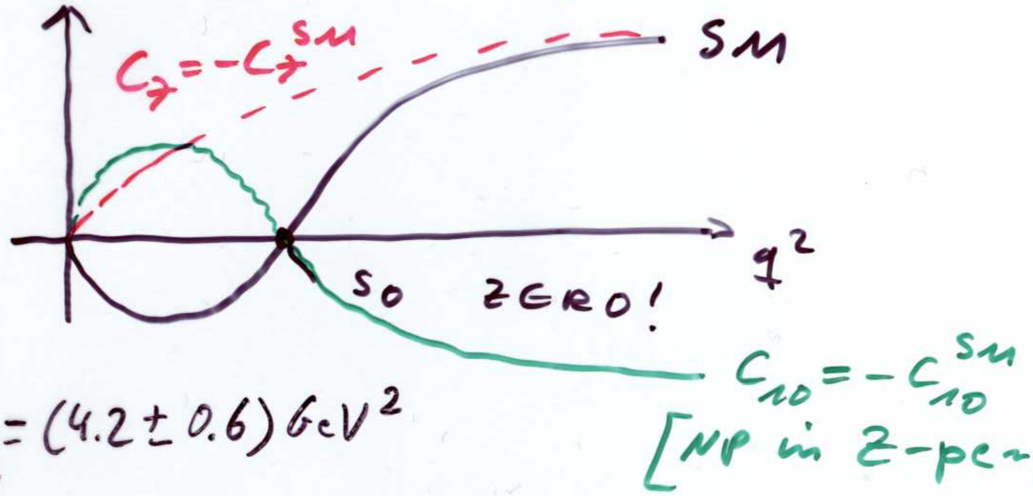

$$s_0(K^*)_{SM} = (4.2 \pm 0.6)\, GeV^2$$

$$A_{FB}(B \to K \mu\mu)_{SM} = \phi$$

non-zero induced by O_S, O_P ! hep-ph/0104284

$$A_{FB}(B \to K \mu\mu) \sim C_S (C_7 + \dots C_9)$$

at most $\mathcal{O}(2\%)$ by todays bound on $B_r(B_s \to \mu^+\mu^-)$

FROM hep-ph/0310219

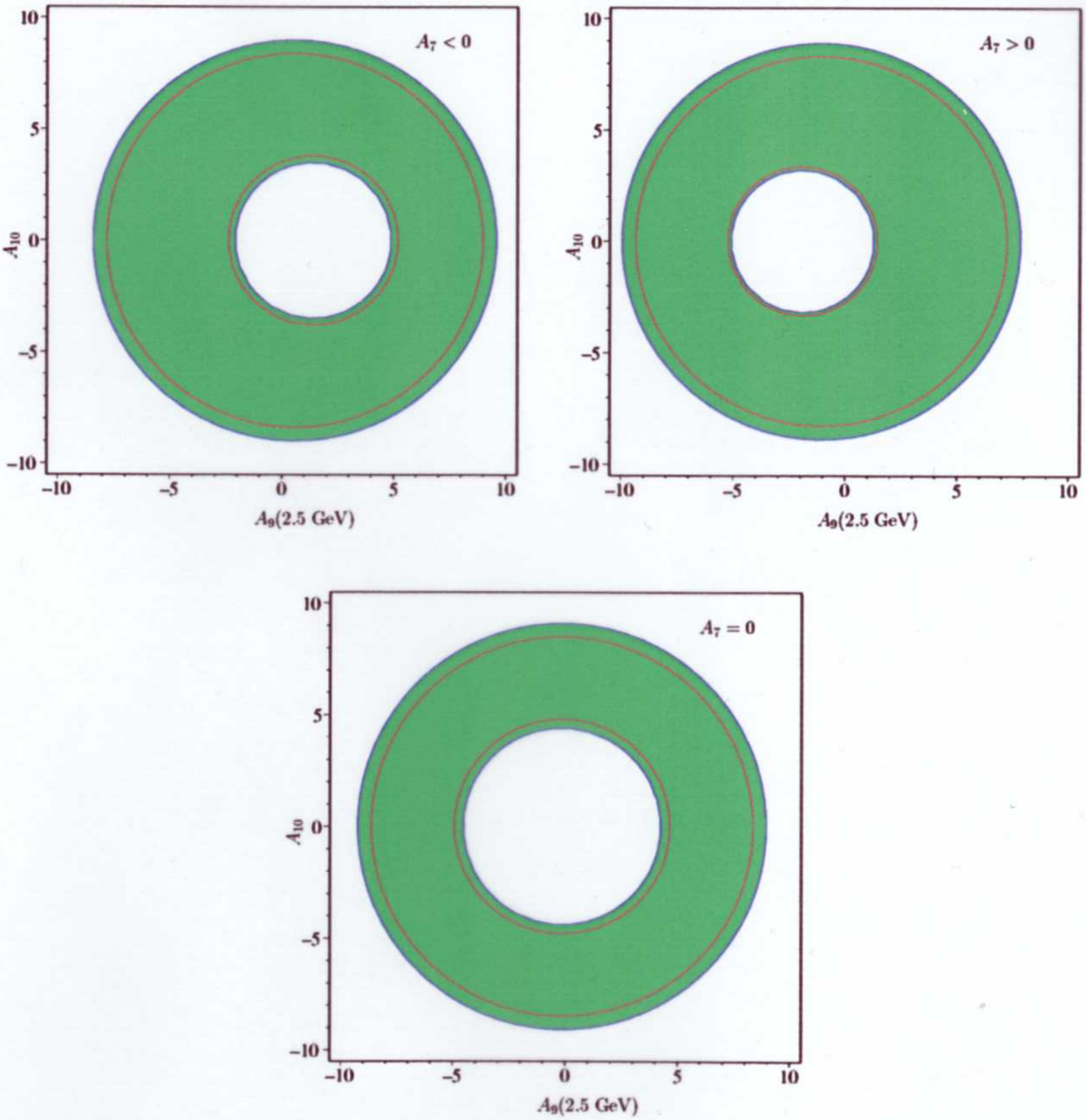

Figure 3: Allowed regions in the A_9–A_{10} plane in the presence of scalar and pseudoscalar operators from data on inclusive $b \to s\ell^+\ell^-$ and $b \to s\gamma$ decays for different values of A_7. The shaded areas are obtained from the upper bound on $\mathcal{B}(B \to X_s e^+ e^-)$ and the lower bound on $\mathcal{B}(B \to X_s \mu^+ \mu^-)$, Eqs. (4.7) and (4.9) with $f_{B_s} = 200$ MeV. The two remaining contours indicate the allowed regions from the 90% C.L. measurement of $\mathcal{B}(B \to X_s e^+ e^-)$ given in Eq. (4.8). Since the bounds from $\mathcal{B}(B \to X_s \mu^+ \mu^-)$ for $f_{B_s} = 238$ MeV give very similar results, we do not show the corresponding contours.